NASA Technical Memorandum 113110 IECEC–97528

Electrical and Optical Performance Characteristics of p/n InGaAs Monolithic Interconnected Modules

David M. Wilt
Lewis Research Center, Cleveland, Ohio

Navid S. Fatemi, Phillip P. Jenkins, Victor G. Weizer,
and Richard W. Hoffman, Jr.
Essential Research, Inc., Cleveland, Ohio

Christopher S. Murray and David R. Riley
Westinghouse Electric Corporation, West Mifflin, Pennsylvania

October 1997

The NASA STI Program Office ... in Profile

Since its founding, NASA has been dedicated to the advancement of aeronautics and space science. The NASA Scientific and Technical Information (STI) Program Office plays a key part in helping NASA maintain this important role.

The NASA STI Program Office is operated by Langley Research Center, the lead center for NASA's scientific and technical information. The NASA STI Program Office provides access to the NASA STI Database, the largest collection of aeronautical and space science STI in the world. The Program Office is also NASA's institutional mechanism for disseminating the results of its research and development activities. These results are published by NASA in the NASA STI Report Series, which includes the following report types:

- TECHNICAL PUBLICATION. Reports of completed research or a major significant phase of research that present the results of NASA programs and include extensive data or theoretical analysis. Includes compilations of significant scientific and technical data and information deemed to be of continuing reference value. NASA counter-part of peer reviewed formal professional papers, but having less stringent limitations on manuscript length and extent of graphic presentations.

- TECHNICAL MEMORANDUM. Scientific and technical findings that are preliminary or of specialized interest, e.g., quick release reports, working papers, and bibliographies that contain minimal annotation. Does not contain extensive analysis.

- CONTRACTOR REPORT. Scientific and technical findings by NASA-sponsored contractors and grantees.

- CONFERENCE PUBLICATION. Collected papers from scientific and technical conferences, symposia, seminars, or other meetings sponsored or co-sponsored by NASA.

- SPECIAL PUBLICATION. Scientific, technical, or historical information from NASA programs, projects, and missions, often concerned with subjects having substantial public interest.

- TECHNICAL TRANSLATION. English-language translations of foreign scientific and technical material pertinent to NASA's mission.

Specialized services that help round out the STI Program Office's diverse offerings include creating custom thesauri, building customized databases, organizing and publishing research results ... even providing videos.

For more information about the NASA STI Program Office, you can:

- Access the NASA STI Program Home Page at http://www.sti.nasa.gov/STI-homepage.html

- E-mail your question via the Internet to help@sti.nasa.gov

- Fax your question to the NASA Access Help Desk at (301) 621-0134

- Phone the NASA Access Help Desk at (301) 621-0390

- Write to:
  NASA Access Help Desk
  NASA Center for AeroSpace Information
  800 Elkridge Landing Road
  Linthicum Heights, MD 21090-2934

NASA Technical Memorandum 113110 IECEC–97528

Electrical and Optical Performance Characteristics of p/n InGaAs Monolithic Interconnected Modules

David M. Wilt
Lewis Research Center, Cleveland, Ohio

Navid S. Fatemi, Phillip P. Jenkins, Victor G. Weizer,
and Richard W. Hoffman, Jr.
Essential Research, Inc., Cleveland, Ohio

Christopher S. Murray and David R. Riley
Westinghouse Electric Corporation, West Mifflin, Pennsylvania

Prepared for the
32nd Intersociety Energy Conversion Engineering Conference
cosponsored by AIChE, ANS, SAE, AIAA, ASME, and IEEE
Honolulu, Hawaii, July 27—August 1, 1997

National Aeronautics and
Space Administration

Lewis Research Center

October 1997

Available from

NASA Center for Aerospace Information
800 Elkridge Landing Road
Linthicum Heights, MD 21090-2934
Price Code: A03

National Technical Information Service
5287 Port Royal Road
Springfield, VA 22100
Price Code: A03

ELECTRICAL AND OPTICAL PERFORMANCE CHARACTERISTICS OF p/n InGaAs MONOLITHIC INTERCONNECTED MODULES

David M. Wilt, Navid S. Fatemi[1], Phillip P. Jenkins[1], Victor G. Weizer[1]
Richard W. Hoffman, Jr.[1], Christopher S. Murray[2] and David R. Riley[2]

NASA Lewis Research Center
21000 Brookpark Rd, M.S. 302-1
Cleveland, Ohio
Phone (216) 433-6293, Fax (216) 433-6106

[1]Essential Research, Inc.
23811 Chagrin Blvd. #220
Cleveland, Ohio
(216) 831-0177

[2]Westinghouse Electric Corporation
P.O. Box 79
West Mifflin, PA

ABSTRACT

There has been a traditional trade-off in thermophotovoltaic (TPV) energy conversion development between system efficiency and power density. This trade-off originates from the use of front surface spectral controls such as selective emitters and various types of filters. A monolithic interconnected module (MIM) structure has been developed which allows for both high power densities and high system efficiencies. The MIM device consists of many individual indium gallium arsenide (InGaAs) devices series-connected on a single semi-insulating indium phosphide (InP) substrate. The MIMs are exposed to the entire emitter output, thereby maximizing output power density. An infrared (IR) reflector placed on the rear surface of the substrate returns the unused portion of the emitter output spectrum back to the emitter for recycling, thereby providing for high system efficiencies.

Initial MIM development has focused on a 1 cm^2 device consisting of eight (8) series interconnected cells. MIM devices, produced from 0.74eV InGaAs, have demonstrated V_{oc} = 3.2 volts, J_{sc} = 70 mA/cm^2 and a fill factor of 66% under flashlamp testing. Infrared (IR) reflectance measurements (> 2 μm) of these devices indicate a reflectivity of > 82%. MIM devices produced from 0.55eV InGaAs have also been demonstrated. In addition, conventional p/n InGaAs devices with record efficiencies (11.7% AM0) have been demonstrated.

INTRODUCTION

In thermophotovoltaic energy conversion, an emitter is heated to incandescence and a photovoltaic device is placed in view of the emitter to convert the radiant energy into electrical energy. Research in TPV has been renewed recently, due to the development of new emitter, filter and photovoltaic cell technology. Most current efforts in TPV research have concentrated on using front surface spectral control elements such as selective emitters [1] or graybody emitters combined with plasma, dielectric or dipole filters [2,3] in order to improve system efficiency to the 20-40% range predicted by theory [4].

The front-surface spectral control approach tends to produce systems with low power density (W/cm^2). Selective emitters, for example, have demonstrated in-band emittances which range from 0.7 to 0.8 [5], with efficiencies of ~40% (i.e. 40% of the emitted energy is convertible by the photovoltaic device). In order to recuperate the non-convertible energy, filters are used to reflect the long-wavelength photons back to the selective emitter. Unfortunately, there are no filters available which provide both 100% transmission in the usable wavelength region and 100% reflection everywhere else. Thus, a selective emitter emitance of 0.8, coupled with a typical filter transmission of 80% leads to a reduction in the power density of 36%. This is an expensive loss, particularly given the cost of TPV cells. Grey body emitter based systems have similar power density problems.

A different approach involves the use of rear-surface spectral controls. Using this technique, the entire radiant output from the emitter is incident upon the photovoltaic (PV) device, thereby providing high output power densities. Photons which the PV device is unable to convert pass through the cell structure, reflect off of a rear reflector and are returned to the emitter for recycling. Researchers have developed TPV cells which utilize low- doped substrates and reflective rear contacts to provide photon recycling [6,7]. Other researchers have developed series-interconnected, monolithic cells

for laser, fiber-optic and TPV applications [8,9]. We are developing a cell which combines the advantages of both of these approaches.

The Monolithic Interconnected Module or MIM consists of series-connected indium gallium arsenide (InGaAs) devices on a common, semi-insulating indium phosphide (InP) substrate (figure 1). An infrared reflector is deposited on the rear surface of the InP substrate to reflect photons back toward the front surface of the cell. This provides a second pass opportunity for photons capable of being converted by the cell. In addition, long wavelength photons are returned to the emitter for "recycling", improving the system efficiency.

concern for electrical isolation. This greatly simplifies the array design and improves the thermal control of the cells. Fourth, the array may easily be designed with differing cell sizes to reduce view factor losses and losses associated with non-uniform emitter temperatures. Last, photons which are weakly absorbed have the possibility of multiple passes through the cell structure. This feature is particularly important for lattice-mismatched devices, where poor minority carrier diffusion length can be partially offset by making the cell thin, forcing the carrier generation to occur closer to the p/n junction.

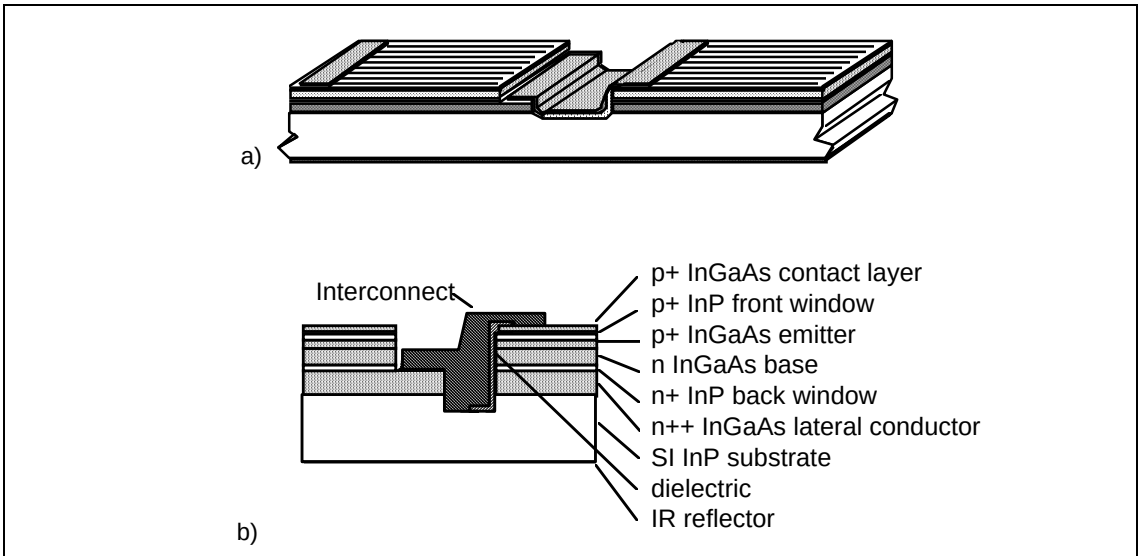

Figure 1. a) A 3- dimensional view of two (2) cells of a MIM. b) A cross-sectional view of a MIM showing the individual layers and interconnect scheme.

The MIM design offers several advantages compared to conventional TPV cell designs. First, small series-connected cells provide high voltages and low currents, thereby reducing I^2R losses. In addition, the small size of the cells allow an array to be comprised of series/parallel strings rather than a single series-connected string of larger cells. This should improve the reliability of the TPV module since the failure of a single cell would not debilitate the entire array. Second, the MIM design maximizes output power density since losses associated with front-surface spectral controls are eliminated.

Third, the rear surface of the device is not electrically active, therefore the cell may be directly bonded to the substrate/heat sink without

MATERIALS DEVELOPMENT

The MIM structures were deposited in a horizontal, low-pressure organo metallic vapor phase epitaxy (OMVPE) reactor described elsewhere [10]. The precursor materials were trimethyl indium (TMIn), trimethyl gallium (TMGa), arsine, phosphine, diethyl zinc (DEZn) and silane for p and n doping respectively. Several test growths were conducted to determine the compositional, thickness and doping uniformity of InGaAs across the 2" diameter substrate. Secondary electron microscopy analysis indicates the thickness variation was +/- 3% in the axial direction and +/- 9% in the perpendicular direction (exclusive of a 5mm wide region at the perimeter of the substrate). These results were consistent from

run to run. Double crystal x-ray rocking curve measurements indicated a variation in InGaAs composition of +/- 0.7% (relative) in the axial direction and +/-0.4% (relative) in the perpendicular direction. This compositional uniformity was reproducible from run to run, although we did observe a variation in the absolute composition of +/- 0.5% In. This was attributed to a variation in the transport efficiency of the TMIn source.

Hall measurements were conducted for both n-type (Si doped) and p-type (Zn doped) InGaAs to map the doping distribution over the 2" diameter substrates. The results indicate a variation of +/- 14% in the axial direction and +/-42% in the perpendicular direction for the n-type material and +/- 2% in the axial direction and +/- 4% in the perpendicular direction for the p-type material. The p-type result is consistent with the compositional and thickness uniformity observed for this sample. The variation observed for the n-type material in the perpendicular direction is believed to be due to enhanced SiH_4 cracking caused by the close proximity of the hot chamber walls. We are examining the use of alternative dopants or modified reactor geometry to reduce this variation.

The MIM device requires dielectric isolation for the interconnect. Three different dielectrics were tested for their suitability. The three materials were e-beam evaporated Ta_2O_5, spin on glass (SOG) and plasma-enhanced chemical vapor deposited (PECVD) Si_3N_4. A test structure was developed to characterize the deposited material for dielectric constant, resistivity and breakdown strength, as well as to test for the presence of pin hole defects. Both the Ta_2O_5 and SOG contained many pinholes and shunting paths. A suitable layer of Si_3N_4 was developed which demonstrated a resistivity of > 10^{10} ohm-cm.

Several different contact and IR reflector metallization materials were tested. The important requirements for these materials were: 1) low specific contact resistance (10^{-6} ohm-cm^2) for both n and p-type InGaAs, 2) good adhesion between the metallization and the InP, InGaAs and the dielectric, and 3) good IR reflection (>95%) for the IR reflector material. The initial tests were conducted with the Au-Ge-Au contacts used in our planar cell development [11]. This material provided excellent contact resistivity and IR reflectivity, but had poor adhesion to the dielectric. We also tested Ag-Au, Cr-Au and Ti-Au and found that the Cr-Au and Ti-Au demonstrated acceptable resistivity (mid 10^{-6} ohm-cm^2) as well as excellent adhesion to the Si_3N_4 and Ta_2O_5 dielectric films and is being used for the MIM contacts. The addition of the Cr sticking layer, however, degraded the IR reflectivity. The devices reported here utilized an Au IR back surface reflector (BSR).

DEVICE DESIGN

A p/n cell configuration (Fig. 1) was chosen for several reasons. First, the free carrier absorption for n-type InGaAs is significantly lower than for p-type, as will be addressed in the following section. Thus, the p/n configuration minimizes the areal density of holes, making it optimum in terms of optical recuperation. Second, the MIM design requires a thick rear conductor layer to conduct current the length of the device (laterally), to reach the back contact/interconnect. The p/n configuration takes advantage of the 25x higher mobility for n-type InGaAs in this conductor layer, reducing the resistive losses.

Finally, an increase in the optical bandgap of the n^{++} conductor layer material (see below) permits the use of a thin base region. Bandedge photons which are not absorbed in the base region are able to pass through the n^{++} layer without being absorbed. These photons reflect off the rear reflector and have a second chance of being absorbed in the base region.

Initial device configurations for both 0.74eV and 0.55eV InGaAs MIM's illuminated by a 1200°K blackbody were developed (fig. 2). The thickness' and doping levels of the lateral conduction layers and emitter layers were chosen to limit the resistive losses to 1% for each layer. The base thickness (2 microns) was intentionally produced for incomplete absorption in a single pass in order to take advantage of the BSR.

The optical efficiency of the 0.74eV MIM device (long wavelength reflectivity) was modeled by determining the free carrier absorption (FCA) for both n and p-type InGaAs as a function of dopant type, level, thickness and wavelength. Calibration samples with doping levels ranging from 5e18 to 3e19 cm^{-3} were fabricated on semi-insulating InP substrates. Absorption measurements were conducted using a spectrophotometer for the near IR (1 - 3 μm) and an FTIR for the mid IR (3 - 10 μm).

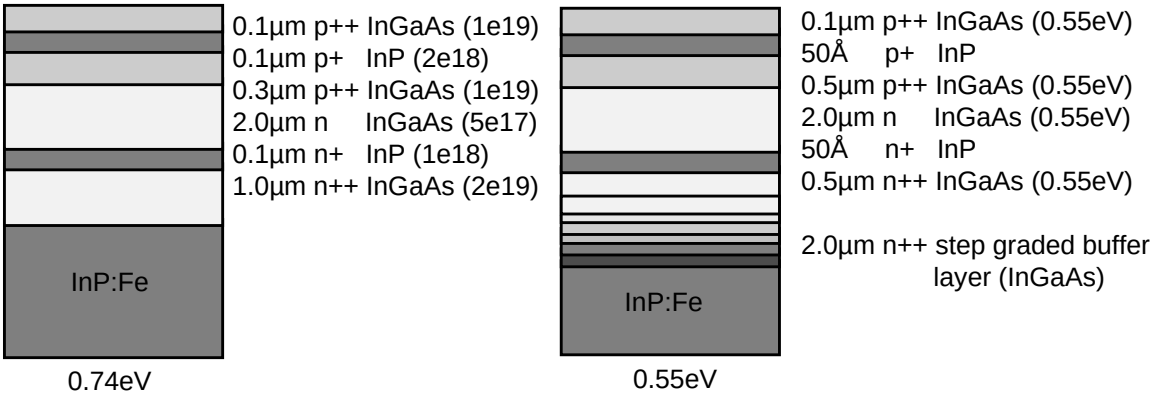

Figure 2. 0.74 and 0.55eV device structures for operation with a 1200K blackbody.

The spectrophotometer absorption data (fig.3) shows several interesting features. First, the absorption for p-type material is significantly higher than for n-type material. Second, the n-type material has an apparent bandgap which is significantly higher (0.3eV) than the equivalent composition p-type material. This shift in absorption is due to a Burstein-Moss shift.

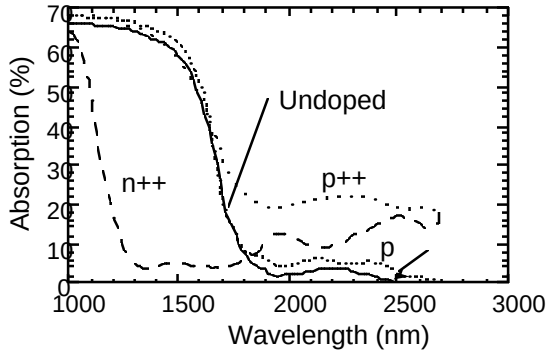

Figure 3. Absorption data for $In_{.55}Ga_{.45}As$ with various doping types and densities.

DEVICE PERFORMANCE

Conventional planar p/n InGaAs devices were produced using the active cell layers shown in figure 2a (note: the emitter doping was reduced to 1e18 cm^{-3} for these devices) in order to verify the basic material quality. The I-V curve shown in figure 4 demonstrates the quality of the baseline devices. The efficiency (11.7% AM0) represents a record for 0.74eV p/n InGaAs. Calculations indicate that reducing the grid shadowing from the 16% on the test device to the 5% normally used in AM0 devices would increase the efficiency to >13%, a record for any 0.74eV InGaAs (p/n or n/p).

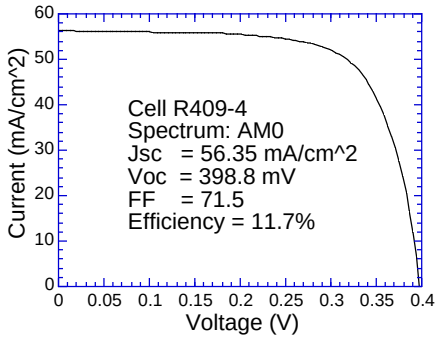

Figure 4. I-V Curve for baseline p/n cell

The external quantum efficiency for a 0.74eV baseline device with a dual layer anti-reflective coating is shown in figure 5. As was stated earlier, the base region was intentionally grown thin so that the effect of the BSR would be demonstrated. It was initially puzzling to observe the high bandedge photoresponse from the conventional cell (with no BSR). Optical modeling indicates that only 62% of the bandedge photons (1600nm) are absorbed in the thin base region, assuming a single pass. Thus, the internal QE could not be greater than 62%. At 1600nm the baseline device demonstrated a 74% internal QE (66% external QE, 10% reflection). The transmission characteristic of a n+ InP substrate was measured at 1600nm and indicated >45% transmission (not corrected for absorption and reflection). Thus, bandedge photons are able to reach the back contact, which is a very reflective, non-alloyed Au based contact. It is believed that this contact acts as a BSR, reflecting the bandedge photons back toward the active cell region. Our past p/n devices had all utilized a sintered contact, which

forms a highly absorbing Au_2P_3 compound at the semiconductor/metal interface. The QE characteristics of these devices did not demonstrate this enhanced bandedge photoresponse.

A negative aspect of this feature is that the reflection is diffuse in nature. Thus non-convertible photons may be totally internally reflected and add to the thermal load of the cell. A benefit of the diffuse reflection is that convertible photons will generally have a longer path length in the active cell layers, improving the probability for absorption. Given the high absorption coefficient for InGaAs, this is a marginal benefit.

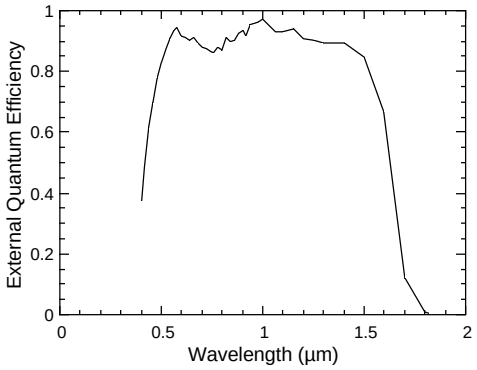

Figure 5. External Quantum Efficiency for the 0.74eV baseline InGaAs device.

The I-V curve for a 0.74eV MIM device is shown in Figure 6 under flashlamp testing. The data indicates an average voltage of 400 mV per cell. This particular device was produced prior to the development of the high quality Si_3N_4 dielectric and, therefore, is not expected to demonstrate optimum performance. The external QE curve for the 0.74eV device is shown in figure 7 (without an anti-reflective coating). The QE data represents the aggregate worst response from across the entire device, given the series interconnected nature of the MIM design. This device is expected to produce 48.5 mA when illuminated by a 1200 K blackbody emitter with a view factor of 1.

A 0.55eV MIM was produced to determine if there were any unforeseen difficulties or problems in producing a MIM from lattice mismatched material. Figure 8 shows the I-V characteristic of a 0.55eV MIM under AM0 testing. As with the 0.74eV device reported above, this cell was produced prior to the optimization of the dielectric material. Unfortunately, this device was destroyed prior to I-V testing at higher injection levels.

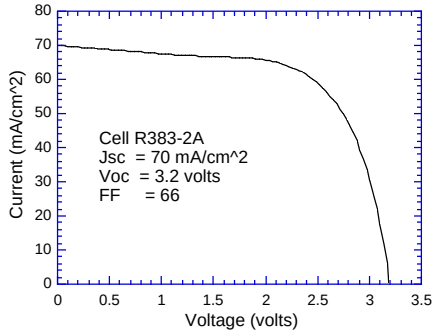

Figure 6. I-V characteristic of 0.74eV MIM under flashlamp testing (10°C).

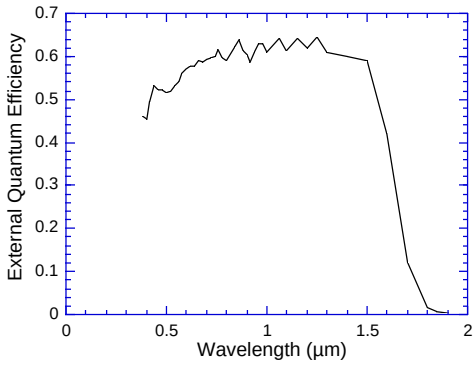

Figure 7. External QE of 0.74eV MIM device without anti-reflective coating.

Figure 9 shows the external QE characteristic for the 0.55eV MIM (without AR). Given the rudimentary nature of the buffer layer used to produce this device and the limited development of the cell layers, the results were very promising.

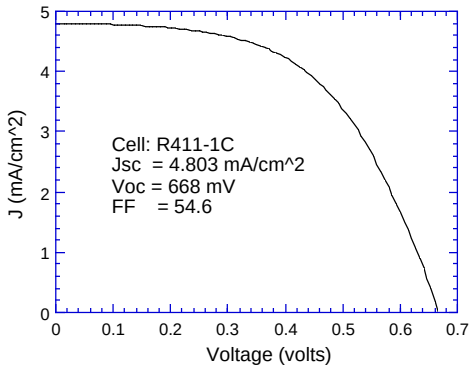

Figure 8. AM0 I-V characteristic of 0.55eV MIM (no AR).

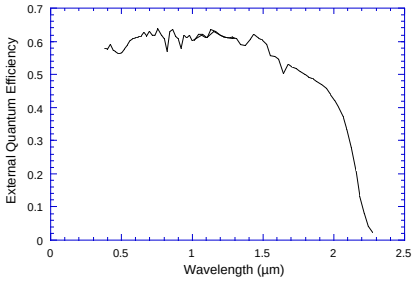

Figure 9. External QE of 0.55eV p/n MIM without AR

Figure 10 shows the measured reflectivity for a 0.74eV MIM device (without an AR coating). This particular device had a 3µm LCL and a low doped emitter (1e18). Optical modeling suggests that IR reflectivity's of >90% are possible with optimized device structures.

The authors wish to acknowledge Dave Scheiman of NASA LeRC for the I-V and QE measurements.

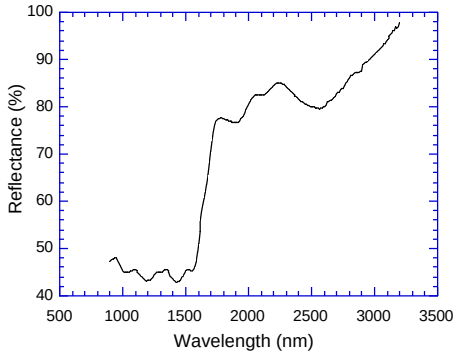

Figure 10. IR reflectance of 0.74eV MIM

REFERENCES

[1] D.L. Chubb and R.L. Lowe, "Thin-Film Selective Emitter", J. Appl. Phys. **79** (9), 1993, pp. 5687-5698.

[2] D.M. Wilt et al., "InGaAs PV Device Development for TPV Power Systems", 1st NREL Conf. on TPV Gen. of Elect., 1994, AIP 321, pp. 210.

[3] W.E. Horne et.al., "IR Filters for TPV Convertor Modules", Proc. 2nd NREL Conf. on TPV Gen. of Elect., 1995, AIP 358, pp. 35.

[4] L.D. Woolf, Solar Cells **19**, 19 (1986).

[5] D.L Chubb et.al., "Review of Recent TPV Research at Lewis Research Center", Proc. 14th SPRAT Conf, 1995, NASA CP-3324, pp. 191.

[6] G.W. Charache et.al., "Thermophotovoltaic Devices Utilizing a Back Surface Reflector for Spectral Control", Proc. 2nd NREL Conf. on TPV Gen. of Elect., 1995, AIP 358, pp. 339.

[7] P.A. Iles and C.L. Chu, "TPV Cells with High BSR", Proc. 2nd NREL Conf. on TPV Gen. of Elect., 1995, AIP 358, pp. 361.

[8] S. Wojtczuk, "Multijunction InGaAs Thermophotovoltaic Power Convertor", Proc. 14th SPRAT Conf, 1995, NASA CP-3324, pp. 223.

[9] M.B. Spitzer et.al., "Monolithic Series-Connected Gallium Arsenide Convertor Development", Proc. IEEE 22nd PVSC, (1991), pp. 142-146.

[10] D.M. Wilt et al., "Monolithically Interconnected InGaAs TPV Module Development", Proc. IEEE 25th PVSC, (1996), pp. 43-48.

[11] D.M. Wilt et.al., "High Efficiency InGaAs Photovoltaic Devices for TPV Power Systems", Appl. Phys. Lett. **64** (18), 1994.

REPORT DOCUMENTATION PAGE

Form Approved
OMB No. 0704-0188

Public reporting burden for this collection of information is estimated to average 1 hour per response, including the time for reviewing instructions, searching existing data sources, gathering and maintaining the data needed, and completing and reviewing the collection of information. Send comments regarding this burden estimate or any other aspect of this collection of information, including suggestions for reducing this burden, to Washington Headquarters Services, Directorate for Information Operations and Reports, 1215 Jefferson Davis Highway, Suite 1204, Arlington, VA 22202-4302, and to the Office of Management and Budget, Paperwork Reduction Project (0704-0188), Washington, DC 20503.

1. AGENCY USE ONLY (*Leave blank*)	2. REPORT DATE	3. REPORT TYPE AND DATES COVERED
	October 1997	Technical Memorandum

4. TITLE AND SUBTITLE

Electrical and Optical Performance Characteristics of p/n InGaAs Monolithic Intereconnected Modules

5. FUNDING NUMBERS

WU–632–1A–1A

6. AUTHOR(S)

Electrical and Optical Performance Characteristics of p/n InGaAs Monolithic Intereconnected Modules

7. PERFORMING ORGANIZATION NAME(S) AND ADDRESS(ES)

National Aeronautics and Space Administration
Lewis Research Center
Cleveland, Ohio 44135–3191

8. PERFORMING ORGANIZATION REPORT NUMBER

E–10866

9. SPONSORING/MONITORING AGENCY NAME(S) AND ADDRESS(ES)

National Aeronautics and Space Administration
Washington, DC 20546–0001

10. SPONSORING/MONITORING AGENCY REPORT NUMBER

NASA TM–113110
IECEC–97528

11. SUPPLEMENTARY NOTES

Prepared for the 32nd Intersociety Energy Conversion Engineering Conference cosponsored by AIChE, ANS, SAE, AIAA, ASME, and IEEE, Honolulu, Hawaii, July 27—August 1, 1997. David M. Wilt, NASA Lewis Research Center; Navid S. Fatemi, Phillip P. Jenkins, Victor G. Weizer, and Richard W. Hoffman, Jr., Essential Research, Inc., Cleveland, Ohio; Christopher S. Murray and David R. Riley, Westinghouse Electric Corporation, West Mifflin, Pennsylvania. Responsible person, David M. Wilt, organization code 5410, (216) 433–6293.

12a. DISTRIBUTION/AVAILABILITY STATEMENT

Unclassified - Unlimited
Subject Categories: 20 and 44 Distribution: Nonstandard

This publication is available from the NASA Center for AeroSpace Information, (301) 621–0390.

12b. DISTRIBUTION CODE

13. ABSTRACT ***(Maximum 200 words)***

There has been a traditional trade-off in thermophotovoltaic (TPV) energy conversion development between system efficiency and power density. This trade-off originates from the use of front surface spectral controls such as selective emitters and various types of filters. A monolithic interconnected module (MIM) structure has been developed which allows for both high power densities and high system efficiencies. The MIM device consists of many individual indium gallium arsenide (InGaAs) devices series-connected on a single semi-insulating indium phosphide (InP) substrate. The MIMs are exposed to the entire emitter output, thereby maximizing output power density. An infrared (IR) reflector placed on the rear surface of the substrate returns the unused portion of the emitter output spectrum back to the emitter for recycling, thereby providing for high system efficiencies. Initial MIM development has focused on a 1 cm^2 device consisting of eight (8) series interconnected cells. MIM devices, produced from 0.74eV InGaAs, have demonstrated V_{∞} = 3.2 volts, J_{sc} = 70 mA/cm^2 and a fill factor of 66% under flashlamp testing. Infrared (IR) reflectance measurements (> 2 μm) of these devices indicate a reflectivity of > 82%. MIM devices produced from 0.55eV InGaAs have also been demonstrated. In addition, conventional p/n InGaAs devices with record efficiencies (11.7% AM0) have been demonstrated.

14. SUBJECT TERMS

Thermophotovoltaics; Indium; Gallium arsenide

15. NUMBER OF PAGES

12

16. PRICE CODE

A03

17. SECURITY CLASSIFICATION OF REPORT	18. SECURITY CLASSIFICATION OF THIS PAGE	19. SECURITY CLASSIFICATION OF ABSTRACT	20. LIMITATION OF ABSTRACT
Unclassified	Unclassified	Unclassified	